CENTRIFUGE MODELLING OF TUNNELLING WITH FOREPOLING

DIVALL, S.[1], TAYLOR, R. N.[1] AND XU, M.[2]

1. City University London, London, UK

2. Chongqing University, Chongqing, China

ABSTRACT

Geotechnical centrifuge modelling provides a means by which geotechnical events and processes can be better understood. In particular, the technique has proved invaluable when investigating collapse mechanisms in small scale models that can be related to full scale events. A series of eight plane strain centrifuge model tests investigating the effect of inserting inclusions around the annulus of a single tunnel in overconsolidated clay has been conducted using the geotechnical centrifuge at City University London. The model used a compressed air supported circular cavity to simulate the tunnel. Stiff resin inclusions embedded around its periphery were used to represent closely spaced forepoles forming grout umbrella arches. Image processing was used to obtain patterns of displacements at the subsurface and displacement transducers measured vertical settlement at the ground surface level. The investigation focused on how different arrangements of forepoling affected tunnel stability. The influence of forepoling on normally accepted plastic collapse mechanisms is discussed. An optimisation of the forepoling layout is suggested in accordance with the findings.

Keywords: Centrifuge modelling, Ground improvement, Tunnels and tunnelling, Ground movements,

Notation

C	depth of tunnel cover
D	tunnel diameter
i	horizontal distance from the tunnel centre line to the point of inflexion on the settlement trough
K	trough width parameter
N_C	critical stability ratio for collapse
S_u	undrained shear strength
S_v	settlement
$S_{v\,max}$	maximum settlement at the tunnel centre line
V_L	volume loss
V_S	volume of the surface settlement trough
V_T	total volume of tunnel
x	horizontal distance from the tunnel centre line
z	depth
z_0	distance from the undeformed surface to tunnel axis level
δ	separation distance from the cavity boundary
γ	unit weight of soil
σ_{TC}	internal tunnel support pressure at collapse

1. INTRODUCTION

In any tunnelling project adequate stability during construction is of prime importance. However, in recent years ground treatment has been undertaken ahead of the face to improve the stability and control ground movements. Construction techniques are conducted to form a pre-lining in unfavourable ground conditions (Mair & Taylor, 1997). Often this technique can take the form of injected grout steel pipes (defined as forepoling by Volkmann & Schubert, 2007) or the installation of bars around the periphery of the face, typically over the upper quarter or third of the excavated profile. In most cases, hollow pipes are used *in lieu* of bars, with grout being injected through the pipes. The insertion angle of the pipes is typically 10° - 30° relative to the tunnel centre-line and excess grout from the apertures forms an equivalent reinforcement area around the tunnel (Figure 1).

Understanding the effect on ground movements arising from this type of construction is necessary to predict the possible settlement damage to both nearby surface and subsurface structures. Asset owners and practitioners alike have driven a requirement for more accurate predictions arising in non-greenfield conditions. However, as a baseline, this study has compared the conventional greenfield tunnelling-induced ground movements with those observed when some form of forepoling support is included.

A series of eight two-dimensional plane strain centrifuge model tests were conducted to investigate how the installation of the ground supports affect the plastic collapse mechanism surrounding a tunnel excavation in firm clay. The model used a compressed air supported circular cavity to simulate the tunnel and stiff resin inclusions were embedded around its periphery. These inclusions were analogous to elements of a secant pipe or forepoling arch system. A consequence of plane strain modelling was that the forepoles were parallel to the tunnel axis. The limitations to this simplification are that the incline of forepoling used in practice was omitted in the model which by its very nature does not simulate the longitudinal settlements along the line of the tunnel.

Seven different layouts of inclusions (forepoling) were investigated and a reference test with no forepoles (Table 1). The premise being tested was whether forepoling embedded around the periphery of the tunnel would provide effective support to the tunnel, thus reducing the potential damage to nearby building foundations and other buried services. By comparing the observed collapse patterns, tunnel stability and patterns of ground movements a feasible optimisation of the layout is suggested.

2. CURRENT UNDERSTANDING OF TUNNEL STABILITY

Although the investigation is primarily concerned with findings useful for pre-collapse ground movements it is still beneficial to understand the failure mechanisms. This is because the patterns of pre-collapse movements are reasonably consistent with overall failure mechanisms (see for example the centrifuge experiments by Mair, 1979).

Investigations have often idealised the tunnelling-induced ground movements into a two-dimensional plane strain scenario (shown in Figure 2). This shows a circular tunnel of diameter, D, at a depth of cover, C in a soil with undrained shear strength, S_u, that is constant with depth. Away from the tunnel face it is reasonable to assume that all the sources of movement are in the plane perpendicular to the tunnel and that the tunnel could be represented to the plane strain conditions (Mair & Taylor, 1997).

Based on a series of centrifuge tests Mair (1979) proposed a critical stability ratio for collapse, N_C. The concept of a stability ratio related the geometric arrangement of the tunnel and support pressure with the undrained strength of the ground.

$$N_C = \frac{\gamma\left(C + {}^{D}/_{2}\right) - \sigma_{TC}}{S_u} \qquad \text{Equation (1)}$$

where: γ is the unit weight of soil and σ_{TC} is the internal tunnel support pressure at collapse.

Davis *et al.* (1980) investigated upper and lower bound solutions for calculating tunnel support pressure with respect to $\gamma D/S_u$ (Figure 3). These two studies were significant in detailing the accepted plastic collapse mechanisms for single greenfield tunnels in clay (Figure 4) and by extension, the patterns of subsurface movements generated during a construction project.

The ground movements resulting from these mechanisms have been shown by many authors (i.e. Peck, 1969; Schmidt, 1989; Mair, 1979; Mair *et al.*, 1993) to be well-described by the Gaussian distribution curve:

$$S_v = S_{v\,max} \exp(-x^2/2i^2) \qquad \text{Equation (2)}$$

where: S_v is settlement, $S_{v\ max}$ is the maximum settlement at the tunnel centre-line, x is the horizontal distance from the tunnel centre-line and *i* is the horizontal distance from the tunnel centre-line to the point of inflexion on the settlement trough. The cross-sectional area of this trough can be defined by:

$$V_S = S_{v\,max}\sqrt{2\pi}\cdot i \qquad \text{Equation (3)}$$

where: V_S is the Volume of the Surface settlement trough. This is often divided by the total Volume of Tunnel, V_T, to give the Volume Loss, V_L.

O'Reilly & New (1982) analysed many case studies which indicated that *i* is related to the tunnel depth as:

$$i = Kz_0 \qquad \text{Equation (4)}$$

where: K is the trough width parameter and z_0 is the distance from the undeformed surface to tunnel axis level. It was further shown that for practical purposes the value for K can be taken as 0.5 for clays.

Mair *et al.* (1993) further analysed case history data and showed that at a depth, z, below the ground surface the trough width parameter, *i*, can be expressed as:

$$i = K(z_0 - z) \qquad \text{Equation (5)}$$

The expression for K then becomes:

$$K = \frac{0.175 + 0.325(1 - z/z_0)}{1 - z/z_o} \qquad \text{Equation (6)}$$

The intention of this study was to assess the effect forepoling has on these ground movements by intersecting the shearing planes in the vicinity of the tunnel shown in Figure 4. Reinforcing the soil or restraining the potential collapse mechanisms could improve the overall stability of the tunnel construction and minimise any ground movements.

3. CENTRIFUGE MODEL TESTS

The centrifuge

Centrifuge modelling techniques as a tool for investigating geotechnical events has been well-documented (Schofield, 1980). This study used the Acutronic 661 geotechnical centrifuge at City University London. It is a beam centrifuge with a radius to the swing bed of 1.8m, and has a typical working radius for soil models tests of 1.65m. A full discussion and schematic of the current facility has been given by Grant (1998), who also described the procedure for modelling tunnelling-induced settlements.

Typical Model Geometry

This study adopted a shallow tunnel arrangement with C/D=2. The tunnel diameter was 50mm and was constant in all tests. A standard plane strain strong box was used which resulted in a model height of 207mm and plan area of 550mm x 200mm. The tunnel axis level was set 79mm from the base of the model (Figure 5). Other centrifuge tests had indicated that this was sufficiently remote from the base of the strong box to avoid adverse boundary effects (Taylor, 1995). The water table was fixed at 10mm below the soil surface in all tests using a simple standpipe arrangement.

The models were tested at 100g, which according to standard scaling laws, represented a 5m diameter tunnel at equivalent prototype scale. Eight different arrangements of model test were devised. The test series contained seven models incorporating forepoling in different geometric arrangements and a reference test with no forepoles (Table 1).

Forepole Geometries

The tests FP2 to FP9 had forepoling embedded around the periphery of the cavity. Fast setting polyurethane resin was found by Gorasia (2013) to be a convenient material for modelling concrete piles and was adopted for the forepoling in these tests. An enlarged diagram of the arrangement for FP3 (in Table 1) is shown in Figure 6 to highlight the key dimensions.

The individual forepoles were designed to have a diameter of 5mm and a separation distance from the cavity boundary, δ, of 5mm. This gave a radius from the centre of the tunnel to the centre of the forepoles of 32.5mm. These were considered acceptable dimensions to conduct the model making processes while also giving reasonable equivalent prototype dimensions.

An amount of overlap between the forepoles was required to form a reinforcement area around the cavity. Adjacent forepoles were offset by a central angle, θ, of 7.5˚ (see Figure 6). This gives a value of centre to centre spacing, *s*, of the forepoles equal to 4.25mm, which was considered to be a sufficient amount of overlap.

Model Preparation

The models were prepared from a slurry of Speswhite kaolin (specific gravity equal to 2.62) mixed at a water content of approximately twice the liquid limit, 120%. The slurry was then placed within a strong-box following commonly adopted practice for model preparation. Full details of this procedure are outlined in Divall & Goodey (2012).

The sample was incrementally one-dimensionally consolidated in the strong box to a maximum vertical effective stress of 350kPa over six days and then swelled back to a pressure of 250kPa for the last 24 hours. This pre-consolidation pressure was chosen to produce a sample of firm clay that would be suitable for investigating tunnel excavation induced ground movements.

At the end of sample consolidation, three Druck PDCR81 miniature pore pressure transducers (PPTs) were inserted via access ports located in the rear of the strong box at depths of 45, 125 and 165mm below the surface. This instrumentation was mainly used to monitor the pore-water pressure as the soil came into effective stress equilibrium on the centrifuge. The transducers were laterally 155mm away from the tunnel centre-line.

On the day of the test the drainage taps were closed and the free water was removed from the inside of the box. The strong-box was moved to the bench where the model was prepared. The front wall of the strong-box was removed and the front of clay sealed with silicone fluid to prevent drying shrinkage. The excess clay was trimmed away from the top surface of the clay to the appropriate height using a specially fabricated guide and sealed again with silicone fluid.

To ensure repeatable boring of the forepoling a special guide was bolted onto the front of the strong box (Figure 7). The guide had 37 holes at a pitch circle radius of 32.5mm (at 7.5° intervals) to direct the boring of the forepoles. Each bore in the clay was conducted using a 5mm diameter thin walled seamless tube and checked to ensure to no excess clay remained inside these cavities. The resin for the forepoling (Biresin G27, Sylmasta Ltd) was mixed with powder filler (JB-FRF5 Filler, Trihydrated Alumina) at a weight proportion of 1:1:2

(resin-A:hardener-B:powder). Laboratory tests on the cast resin indicated strengths in the range 20 to 25MPa and stiffness of approximately 800MPa (McNamara, 2001). The resin was injected into the cavities using a syringe and began to harden after about two minutes. It reached full strength in approximately 30 minutes. Although this method of creating forepoles differs from that used in practice, it was found to give consistent results and post-test investigation indicated good adhesion between the resin and clay sample.

Subsequently, the rest of the sample preparation followed commonly adopted practice for tunnel models (Grant & Taylor, 2000 or Divall & Goodey, 2012). The forepoling guide was removed and a tunnel cutter guide was bolted onto the front of the model. A circular cavity was bored using a previously lubricated, 50mm diameter, thin walled stainless steel tube and a 0.75 mm thick latex bag with a brass union was placed within.

The required image processing marker beads (3mm diameter black cylinders) were pressed into the front clay surface for monitor subsurface displacements and an 83mm thick poly(methyl) methacrylate (PMMA) observation window bolted to the box (Figure 8). Twelve Linear Variable Differential Transformers (LVDTs) were mounted on a gantry above the model for monitoring the surface displacements. These were spaced at 45mm centres from the centre-line of the model. This completed the sample preparation. The model was then placed on the centrifuge swing and a pressure transducer screwed onto a specially designed union (Grant, 1998) to supply compressed air to the latex bag through the back wall of the strong-box. 450ml silicone oil was poured onto the top surface to prevent evaporation of pore water from the clay during the test. Once the power supplies and transducers were connected the final checks were made and the test commenced. During the centrifuge acceleration phase, the air pressure inside the cavity was increased progressively to balance the increasing overburden stress at the tunnel axis level.

Test Procedure

After the acceleration had reached 100g the model was allowed to reach hydrostatic equilibrium. In this phase, the average soil settlement was about 0.2mm and thus small relative to the size of sample. That the forepoles had been placed prior to the consolidation phase was considered to have minimal effect on the overall observed behaviour. The model was judged to have reached effective stress equilibrium by careful inspection of the PPT data; this phase took approximately 24 hours. After the equilibrium was reached, the excavation was simulated by reducing the air-pressure (from an average initial support pressure of

211kPa) at the rate of about 100kPa per minute, thus achieving an undrained event. During this phase, data were recorded every second and pictures of the model were stored at approximately one second intervals.

Post-test Procedure

The undrained shear strength was obtained from each model using a Pilcon hand shear vane immediately after the centrifuge had been stopped. Usually two or three sites were selected and strength measured at up to five depths. Table 2 shows the results from this procedure.

Once the models were removed from the swing, the model could be dissected and the resin forepoles inspected for quality of casting. Figure 9 shows the resin forepoling after removal from the clay model for arrangements FP2, FP3, FP4 and FP5. In most cases the casting was of good quality for the entire width of the model. The individual forepoles can be traced from front to rear with only a few instances of cavities merging at the rear of the model. In FP4 and FP5 the collapse mechanism has caused the forepoling to fail longitudinally. In FP4 the failure point was on the centre-line above the tunnel and in FP5 there were two failure points evident at 45° from the tunnel centre-line.

4. RESULTS

The series of single tunnel tests were performed to assess the effect forepoling had on the stability and the subsequent ground movements. While a large quantity of data were obtained from each test only the surface and subsurface settlements and tunnel support pressures are discussed here. This allows for a comparison to be drawn with other published and commonly accepted parameters.

Stability

Figure 10 shows the recorded tunnel support pressures, σ_T, against the measured maximum vertical surface settlements, $S_{v\ max}$. It can be seen that, in all arrangements, the addition of forepoles decreased the support pressure required for an equal amount of settlement. This decrease in support pressure was between 30kPa (FP3) and 70kPa (FP5) immediately before collapse. Figure 10 shows three different trends during the simulated tunnel excavation. FP2, FP3, FP8 and FP9 show tunnelling-induced settlements similar in shape to those of the reference test, FP6. One of the arrangements with the most amount of protection, FP7, collapses suddenly and from a relatively small amount of Volume Loss. However, Figure 10 does not take into account the various undrained shear strengths measured in the models. This is considered reasonable due to the consistency of measured strengths indicated in Table 2.

The stability of each arrangement was quantified using the critical stability ratio relationship by Mair (1979). This relationship uses values for the weight of soil above a tunnel, the supporting tunnel pressure and the undrained shear strength of the soil. The measured undrained shear strengths at tunnel axis level and the tunnel support pressure immediately before collapse were used with Equation 1 to find a value, N_{TC}, for each arrangement (see Table 1). For a circular unlined two-dimensional tunnel the critical stability ratio is approximately 4, Mair (1979). The reference test, FP6, gave a value of 4.1; indicating that the reference test was reproducing tunnelling-induced behaviour as expected. Figure 11 is a 'radar chart' showing the stability ratio value (radial axis) for each arrangement at the position of the forepoling around the tunnel annulus (circumferential axis). Most notably, this plot shows that protecting the annulus of a tunnel between the spring line and 45° is more effective than protecting the crown or invert. In the case of FP4, where the entire top half was protected, N_{TC} was almost identical to FP2. As expected, in the arrangements where the

majority of the annulus is protected, N_{TC} has increased dramatically. FP2, FP3 and FP4 have an increased stability of approximately 8% and FP5 has an increased stability of 30%.

Settlement

The ability to describe accurately tunnelling-induced settlements modified by forepoling inclusions is important for understanding settlement effects in nearby infrastructure. It could also provide valuable insight into the improvements in stability.

Gaussian curves were fitted to the settlement data obtained during the centrifuge experiments in order to compare the shapes of the settlement troughs with published parameters. Jones & Clayton (2012) and Divall (2013) successfully utilised a version of the nonlinear regression method to establish values for comparison from tunnelling-induced settlement data. Essentially, this method calculates the squared sum of the residuals between discrete points (relative to the tunnel centre-line) and points on a settlement curve. Equation (2) and Equation (4) can be used to describe a Gaussian curve and by modifying the parameters i and $S_{v\ max}$ the value of the residuals is minimised to give the closest mathematical fit. Gaussian curves were fitted to the LVDT measurements to create a surface settlement trough. Gaussian curves were also fitted to the image processing data to create subsurface settlement troughs for depths 5mm to 95mm. This provided the values of the points of inflexion, i, with depth, z.

In addition, Grant & Taylor (2000) proposed a vector focus for settlements which would be a point directly below the tunnel centre-line. This vector focus could be obtained by calculating a vector from each target's vertical and horizontal movements (in the image analysis data) and extrapolating to the tunnel centre-line. Analysis of all the depths shows vector foci diverging on a single point. In each arrangement the inflexion points and vector focus could be plotted on axes of i and z, normalised against depth to tunnel axis level, z_0, (Figures 12 – 18). Also included within these figures are the lines representing the reference test and theoretical trend first postulated by Mair *et al.* (1993).

It can be seen for example from test FP3 (Figure 13) that simply protecting the crown has little effect on the distribution of movement around the tunnel relative to the non-forepoling case. It appears that there needs to be a combination of forepoling across the crown and extending to the spring line and beyond to cause the focal point of vectors to be lowered relative to the non-forepoling case. Thus, for tests FP4 and FP5 the ground

movements above the crown horizon were predominately vertical, forcing soil to squeeze into the invert as failure occurs.

An interesting observation is that the only tests to give significant widening of the settlement trough is FP2 and FP9 which had to separate zone of forepoles positioned specifically to resist a Davis *et al*. (1980) mechanism type B or C from developing (see Figure 4). The positioning of the forepoles in these tests appears to have had the effect of both widening the deformation mechanism and consequently the collapse mechanism.

The implication of this is the effect that the introduction of forepoles has on buildings or buried services in the region of potential settlements. In the arrangements where the settlement troughs have been widened (i.e. FP2 and FP9) there could be less differential settlement for a building above the tunnel with a consequent reduction in potential damage.

5. CONCLUSIONS

A series of eight two-dimensional plane strain centrifuge model tests was conducted to investigate how the installation of various configurations of ground support by means of forepoling affects the plastic collapse mechanism surrounding a tunnel excavation in firm clay. These inclusions were analogous to elements of a secant pipe or forepole arch system (Table 1). The effectiveness of forepoles embedded around the periphery of the tunnel in providing support to a tunnel has been discussed.

The key findings are:

- Strategic positioning of inclusions so as to interfere directly with the formation of a plastic collapse mechanism (e.g. FP2 and FP9) gives both a significant increase in stability and widening of the settlement trough.
- Protecting the crown or invert zones alone had little overall affect, unless the inclusions extend to at least the spring line and preferably beyond. Having this type of extensive inclusion results in movements above the crown level becoming predominately vertical (i.e. horizontal movements are effectively reduced).

These tests have investigated tunnels with C/D=2. Further research is needed on tunnels with different C/D ratios, which have inherently different plastic failure mechanisms to see how the positioning of forepole inclusions can be optimised for maximum effect.

ACKNOWLEDGEMENTS

The authors are grateful to Rashik Bhandari for his assistance in validating some of the subsurface values. In addition particular thanks go to colleagues in the Research Centre for Multi-scale Geotechnical Engineering at City University London for their support and guidance.

REFERENCES

Davis, E. H., Gunn, M. J., Mair, R. J. and Seneviratne, H. N. (1980) *The stability of shallow tunnels and underground openings in cohesive material,* Géotechnique, Vol. 30, No. 4, pp. 397-416

Divall, S. and Goodey, R.J. (2012) *Apparatus for centrifuge modelling of sequential twin-tunnel construction,* International Journal of Physical Modelling in Geotechnics, Vol. 12, No. 3, pp. 102-111

Divall, S. (2013) *Ground movements associated with twin-tunnel construction in clay,* Ph.D. Thesis, City University London, London, UK

Gorasia, R.J. (2013) *Behaviour of ribbed piles in clay*, Ph.D. Thesis, City University London

Grant, R. J. and Taylor, R. N. (2000) *Tunnelling-induced ground movements in clay,* Proceedings of the Institution of Civil Engineers, Geotechnical Engineering, London, England, Vol.143, No. 1, pp. 43-55

Grant, R. J. (1998) *Movements around a tunnel in two-layer ground,* Ph.D. Thesis, City University London, London, UK

Mair, R. J. and Taylor, R. N. (1997) *Bored tunnelling in the urban environment,* Proceedings of the 14th International Conference on Soil Mechanics and Foundation Engineering, Vol. 4, Hamburg, Germany, pp. 2353-2385

Mair, R. J., Taylor, R. N. and Bracegirdle, A. (1993) *Subsurface settlement profiles above tunnels in Clays,* Géotechnique, Vol.43, No.2, pp. 315-320

Mair, R. J. (1979) *Centrifugal Modelling of Tunnel Construction in Soft Clay*, Ph.D. Thesis, Cambridge University, Cambridge, UK

McNamara, A.M. (2001) *Influence of heave reducing piles on ground movements around excavations,* Ph.D. Thesis, City University London, London, UK

Schofield, A. N. (1980) *Cambridge University geotechnical centrifuge operations - Rankine lecture,* Géotechnique, Vol. 30, No. 3, pp. 227-268

Taylor, R. N. (1995) *Centrifuges in modelling: principles and scale effects*, In Geotechnical Centrifuge Technology (Taylor, R. N. (ed.)). Blackie Academic & Professional, Glasgow, UK, pp. 19-33

Jones, B. D. and Clayton, C. R. I. (2012) *Surface settlements due to deep tunnels in clay*, London: ICE Research and Development Enabling Fund Grant 1021, Funder's Report, Document No. 1021 03

O'Reilly, M. P. and New, B. M. (1982) *Settlements above tunnels in the United Kingdom – their magnitude and prediction*, Tunnelling '82, Papers Presented at the 3rd International Symposium, Institute of Mining and Metallurgy, London, England, pp. 173-181

Peck, R. B. (1969) *Deep excavation and tunnelling in soft ground*, Proceedings of the 7th International Conference on Soil Mechanics and Foundation Engineering, Mexico City, Mexico, Vol.3, pp. 225-290

Schmidt, B. (1989) *Consolidation settlements due to soft ground tunnelling*, 12th International Conference on Soil Mechanics and Foundation Engineering, Rio, Brazil, Vol. 2, pp. 797-800

Volkmann, G. M. and Schubert, W. (2007) *Geotechnical Model for Pipe Roof Supports in Tunnelling*, Proceedings of the 33rd ITA-AITES World Tunnelling Congress, Underground Space - the 4th Dimension of Metropolises, Prague, Czech Republic, Vol. 1, pp. 755-760

TABLES

Test	σ_v'(kPa)	C/D	θ (°)	No. forepoles	Forepoling Coverage	N_{TC}
FP6	350	2	-	-	-	4.12
FP2			7.5	14	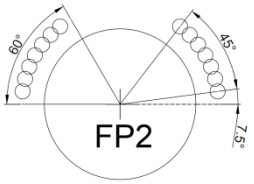	4.45
FP3				15	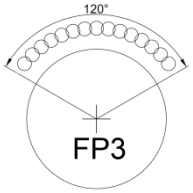	4.31
FP4				25	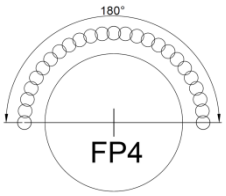	4.44
FP5				37	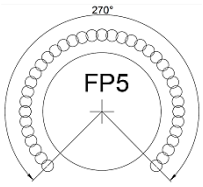	5.36
FP7				37	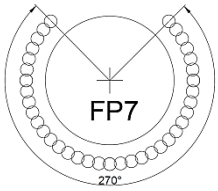	4.90
FP8				25	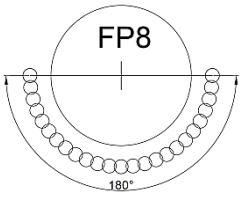	4.21

FP9				26	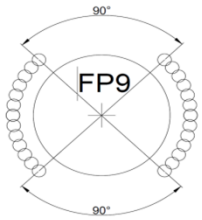	4.94

Table 1: Arrangements for the tests performed

Test ID	S_u Average (kPa)	S_u at Tunnel axis level (kPa)
FP6	32.8	39.0
FP2	33.7	39.3
FP3	30.7	39.0
FP4	35.0	40.7
FP5	34.3	39.6
FP7	33.1	39.6
FP8	32.1	40.0
FP9	35.3	39.9

Table 2: Undrained shear strengths obtained from each arrangement tested

FIGURES

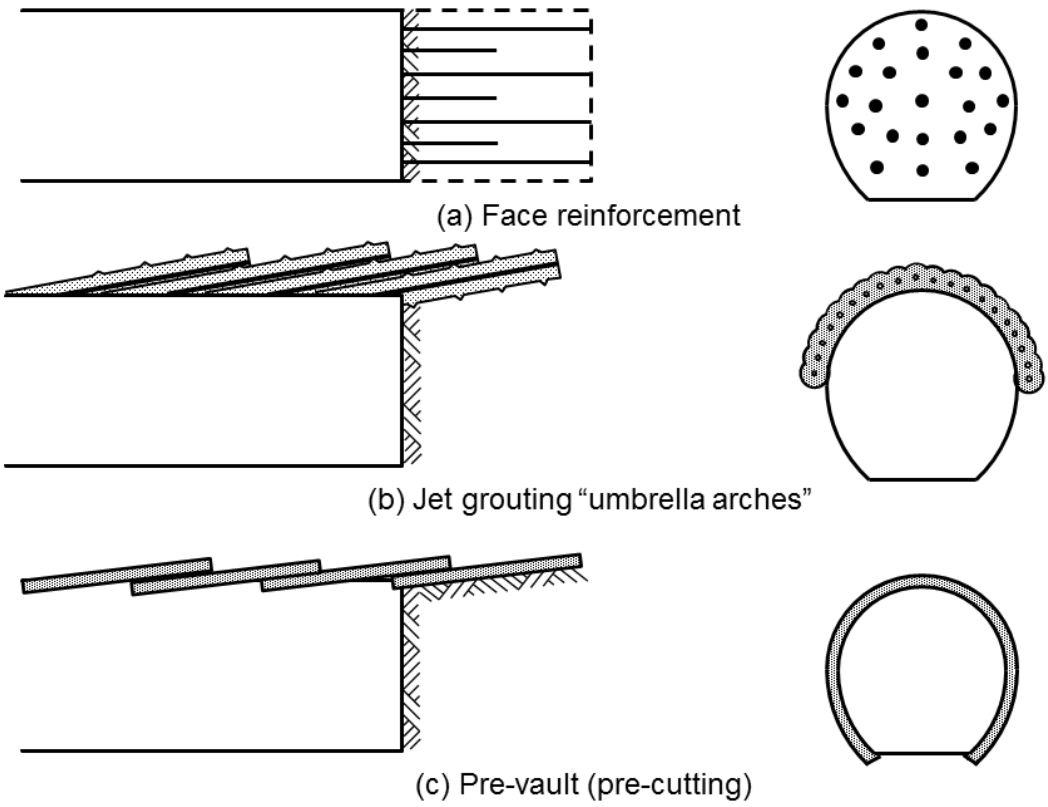

Figure 1: Ground treatment and pre-lining techniques (after Mair & Taylor, 1997)

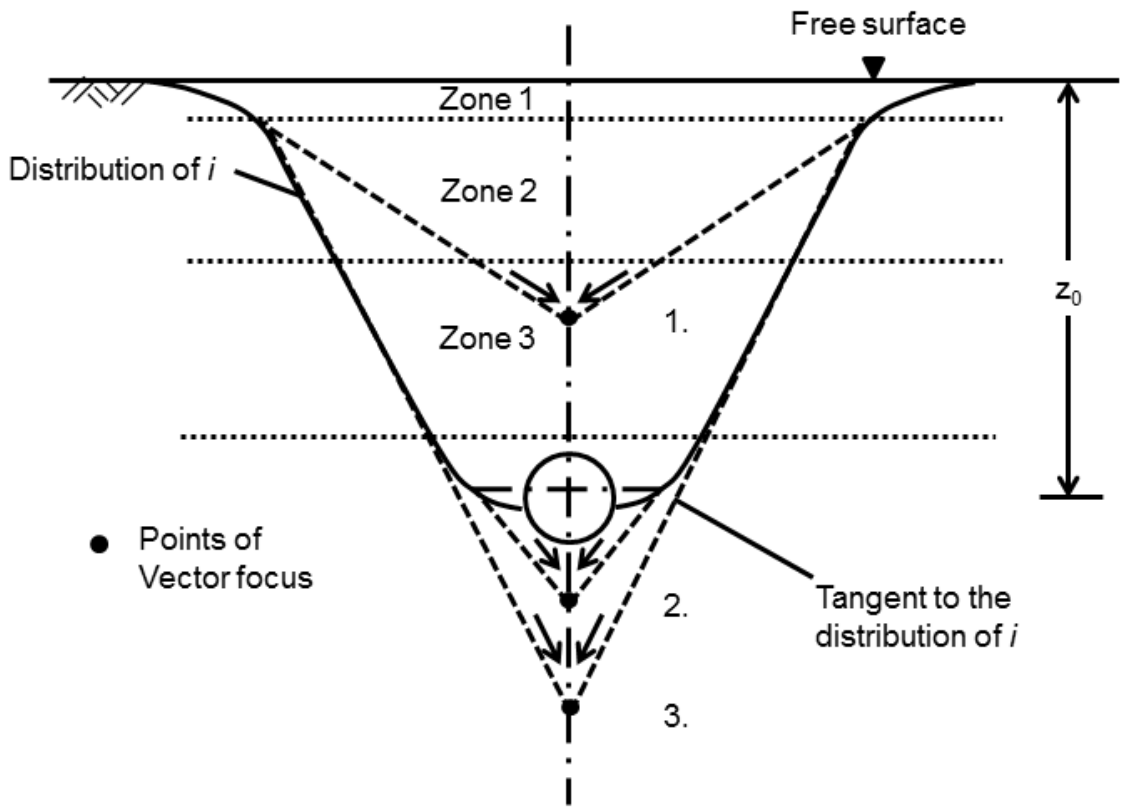

Figure 2: Plane strain tunneling-induced ground movements (after Grant, 1998)

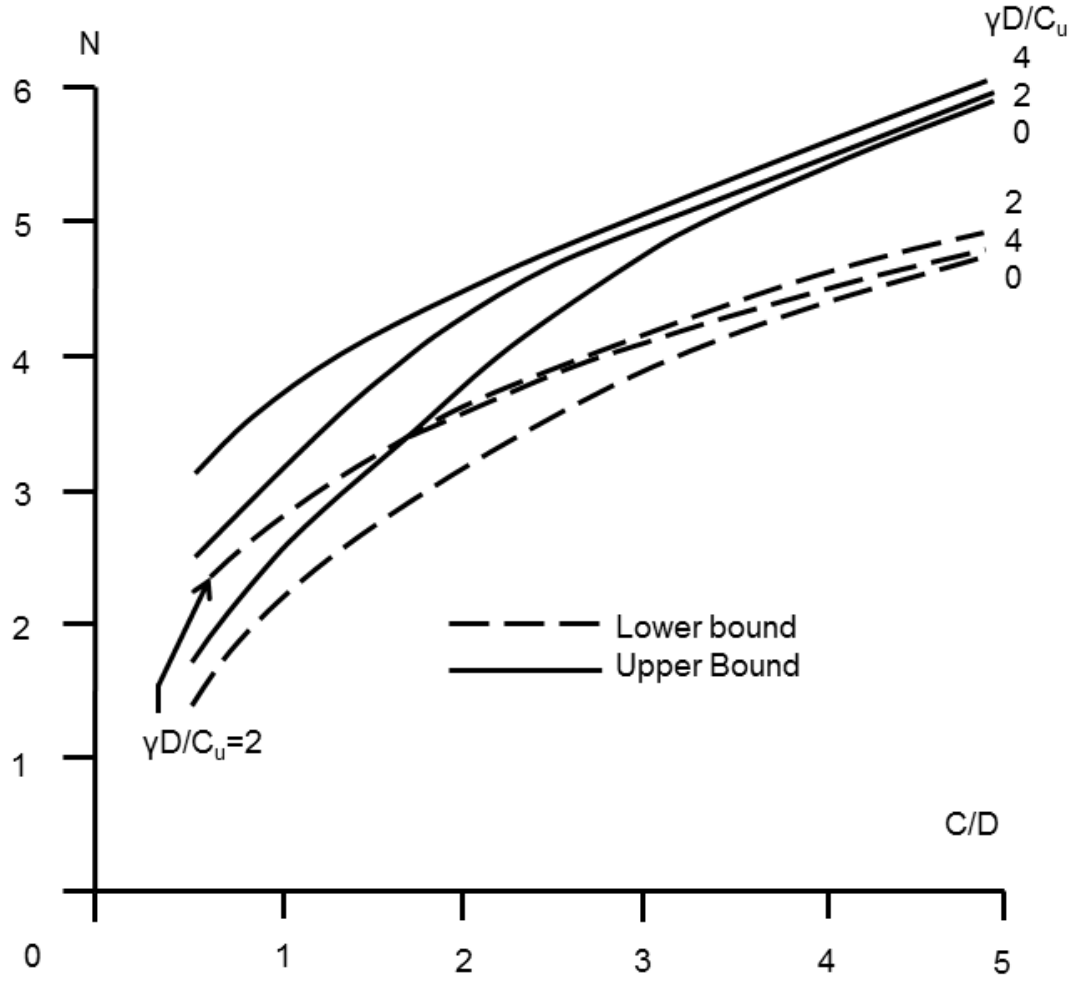

Figure 3: Relationship between stability and soil strength (after, Davis *et al.*, 1980)

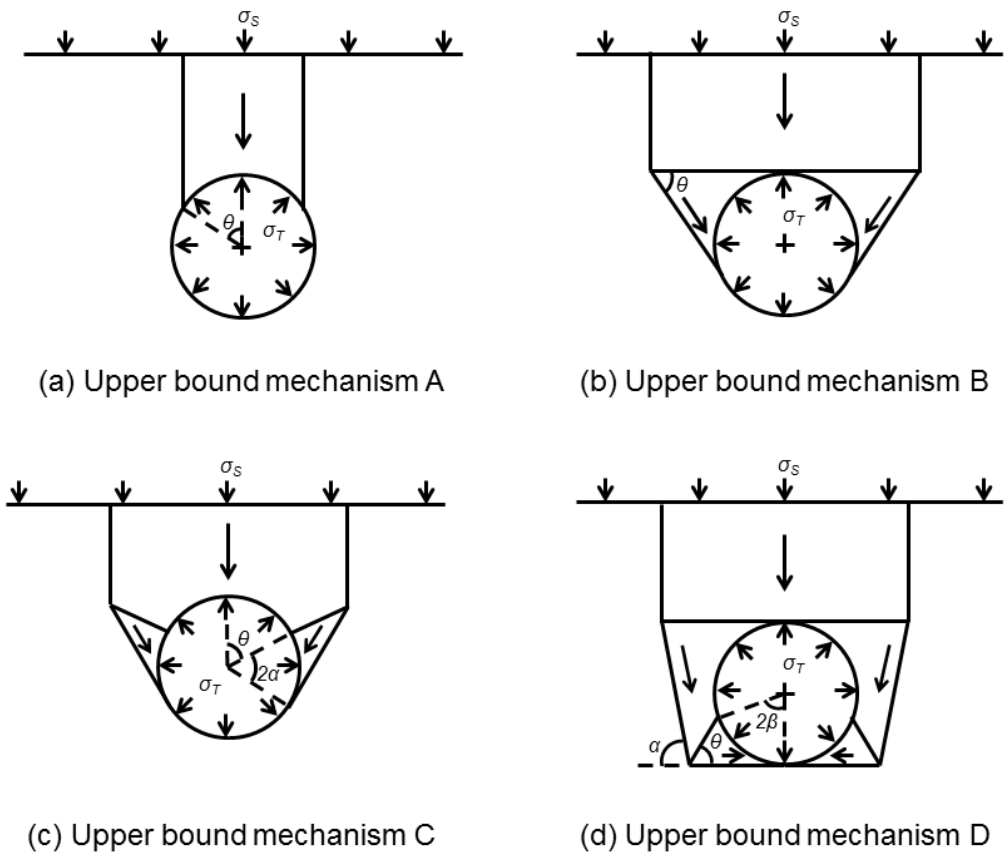

Figure 4: Upper bound mechanisms for plane strain tunneling-induced ground movements (after Davis *et al*., 1980)

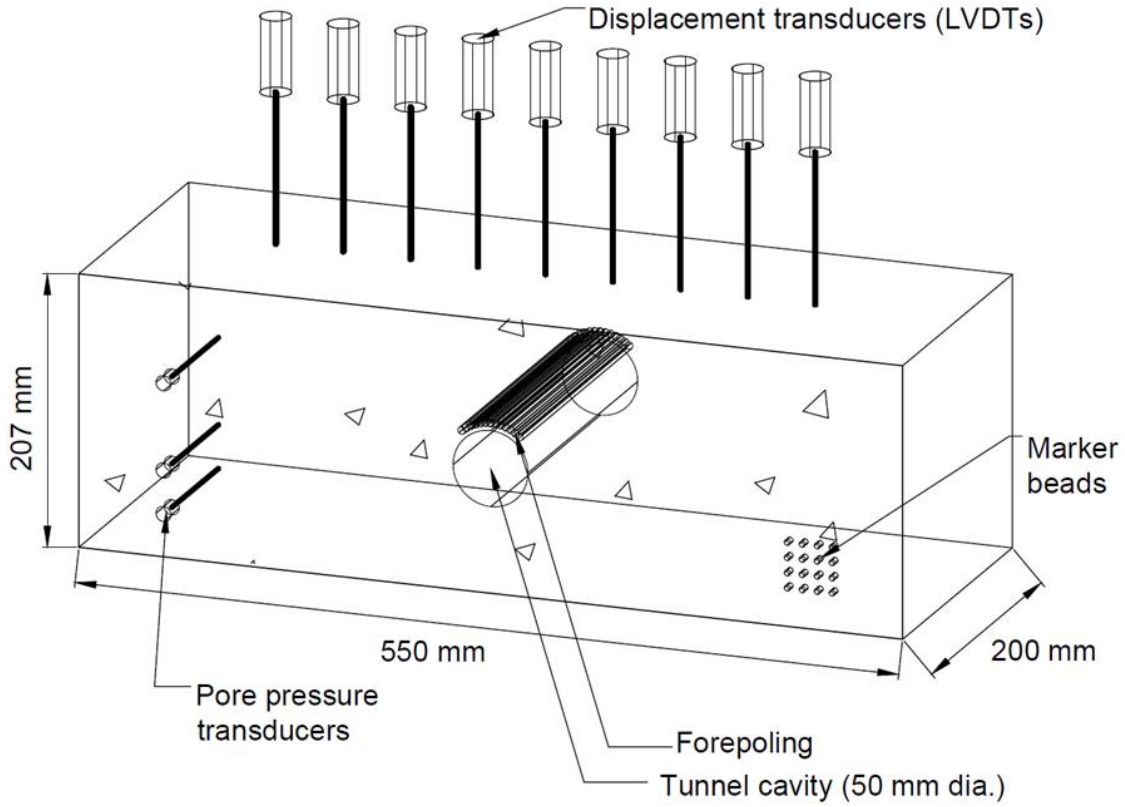

Figure 5: Schematic of the forepoles geometry and location in Test FP3. All the dimensions are given in mm (Not to scale)

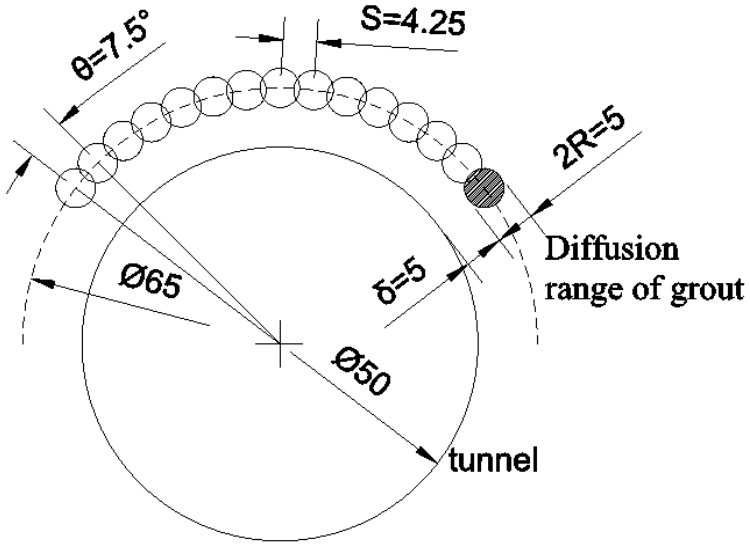

Figure 6: Key dimensions of a forepoling arrangement

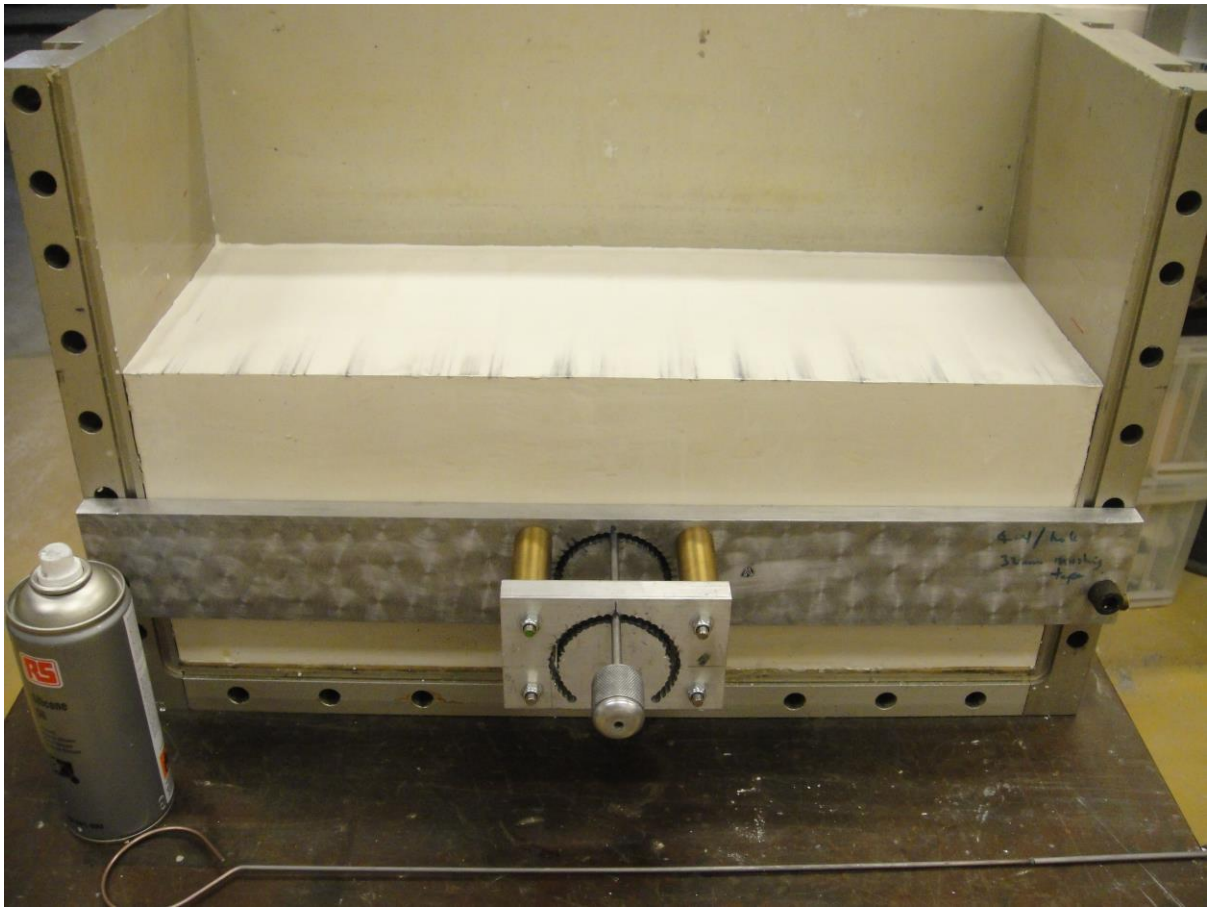

Figure 7: Forepole cavity guide and cutter

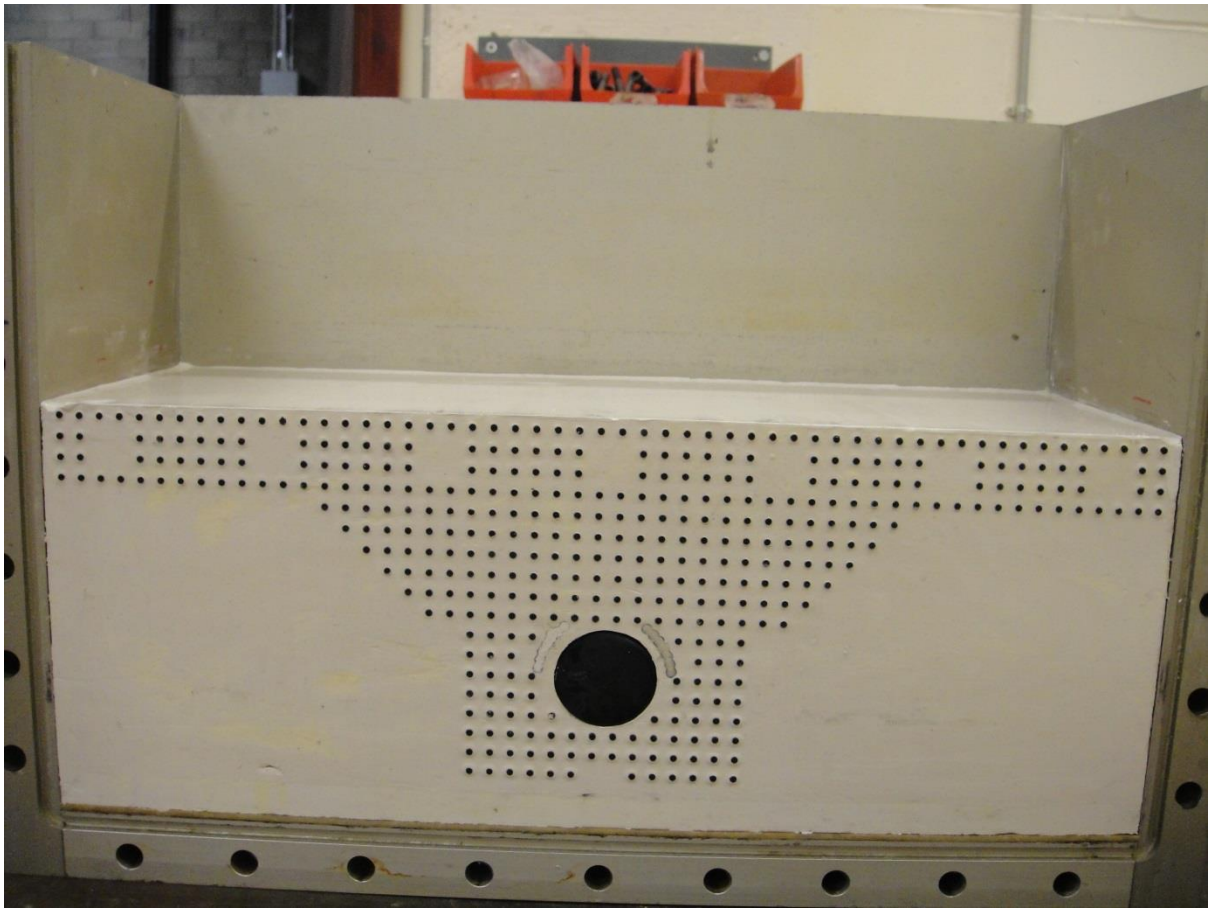

Figure 8: Model complete with latex tunnel membrane, image analysis targets and resin forepoles

Figure 9: Quality of forepoling pouring and casting procedure (length of forpoles 200mm)

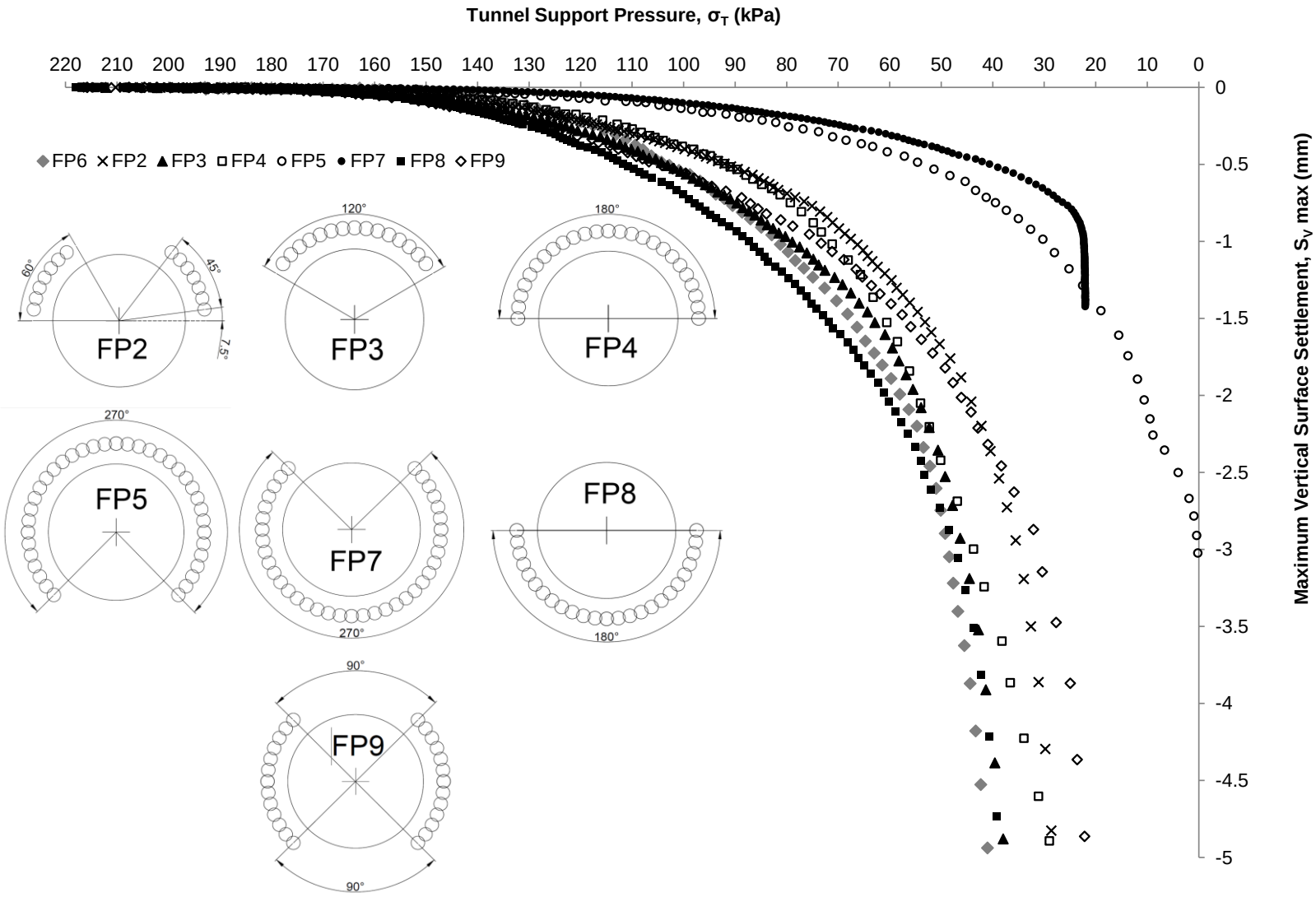

Figure 10: Tunnel pressure against Maximum vertical surface settlement for all forepoling arrangements

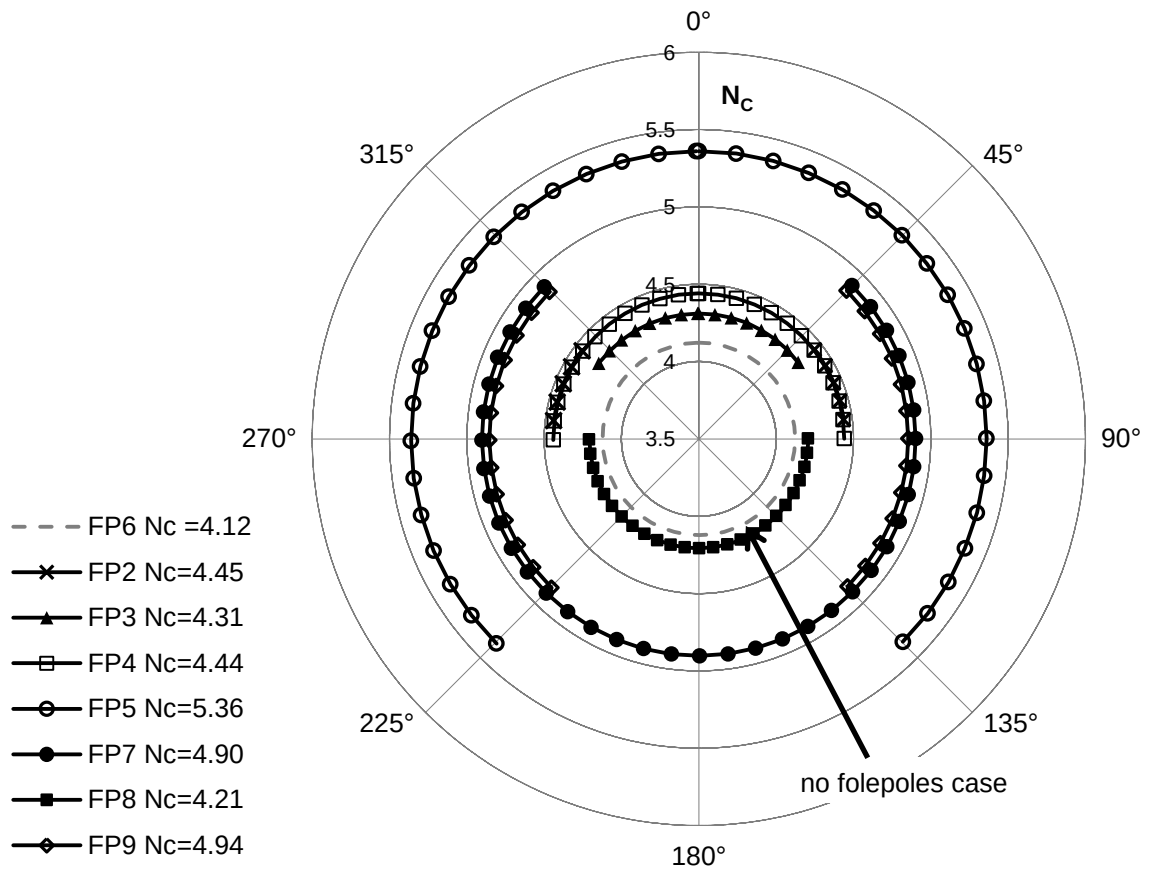

Figure 11: Stability ratio against forepoling position for each arrangement

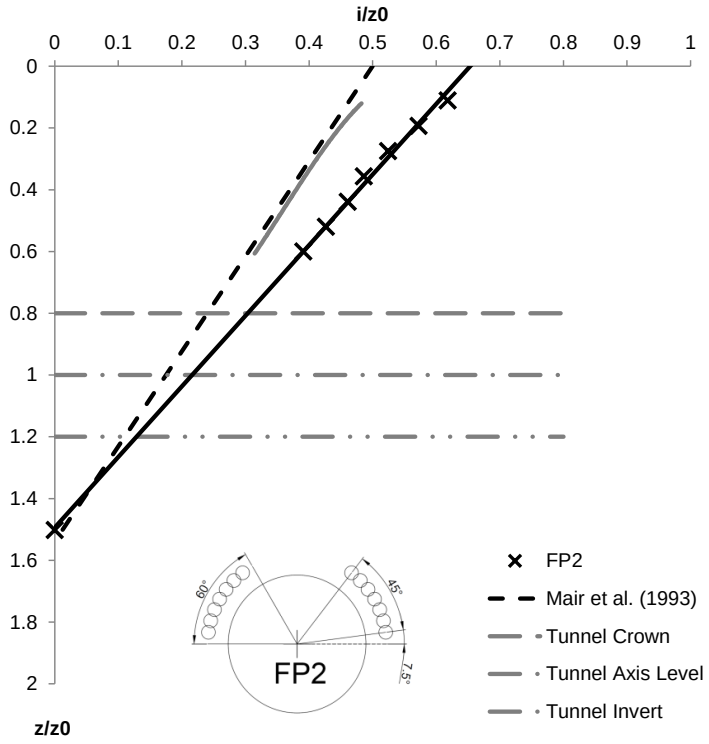

Figure 12: Patterns of deformations with depth for FP2 against theoretical and reference test values

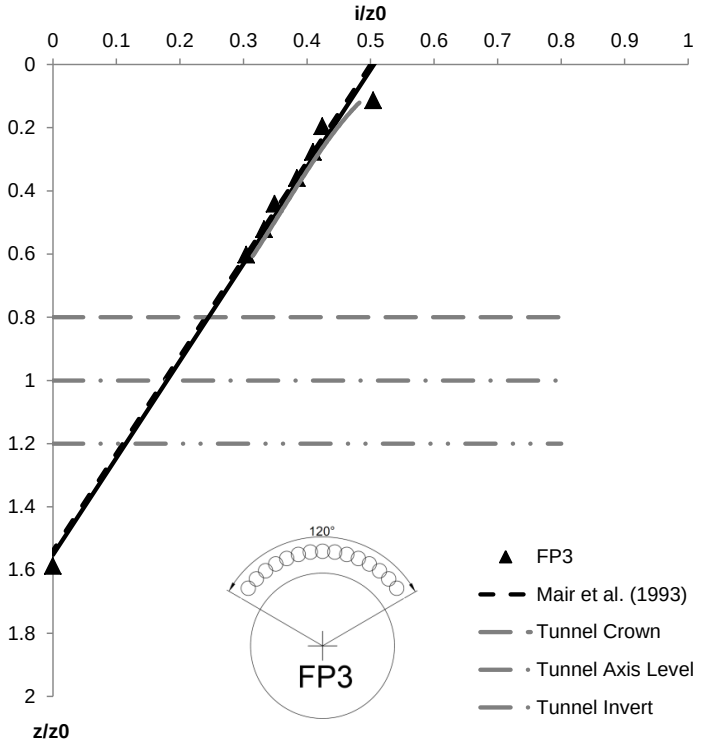

Figure 13: Patterns of deformations with depth for FP3 against theoretical and reference test values

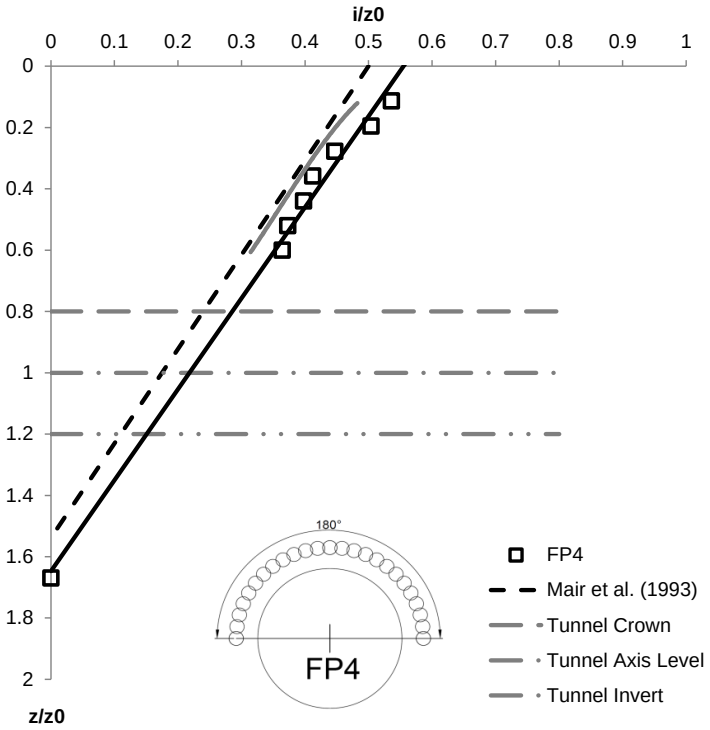

Figure 14: Patterns of deformations with depth for FP4 against theoretical and reference test values

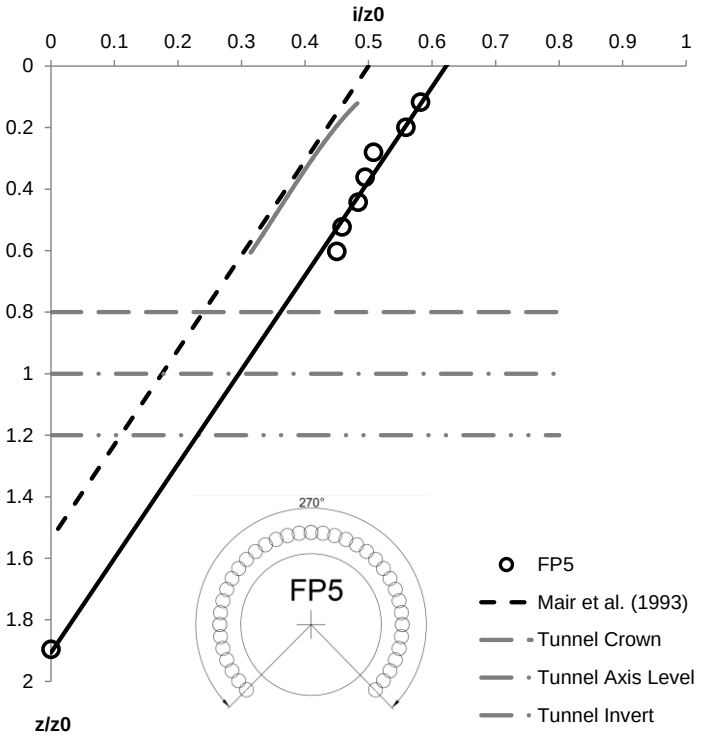

Figure 15: Patterns of deformations with depth for FP5 against theoretical and reference test values

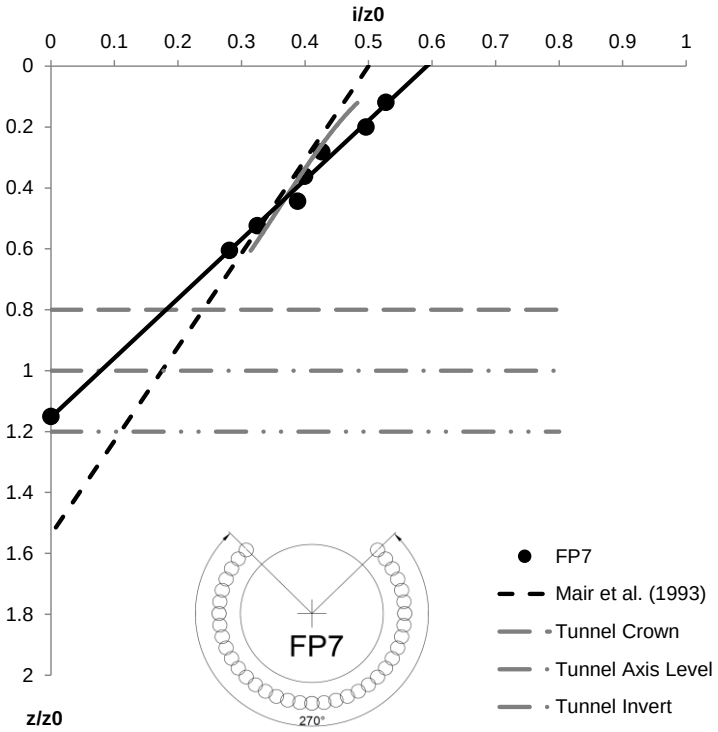

Figure 16: Patterns of deformations with depth for FP7 against theoretical and reference test values

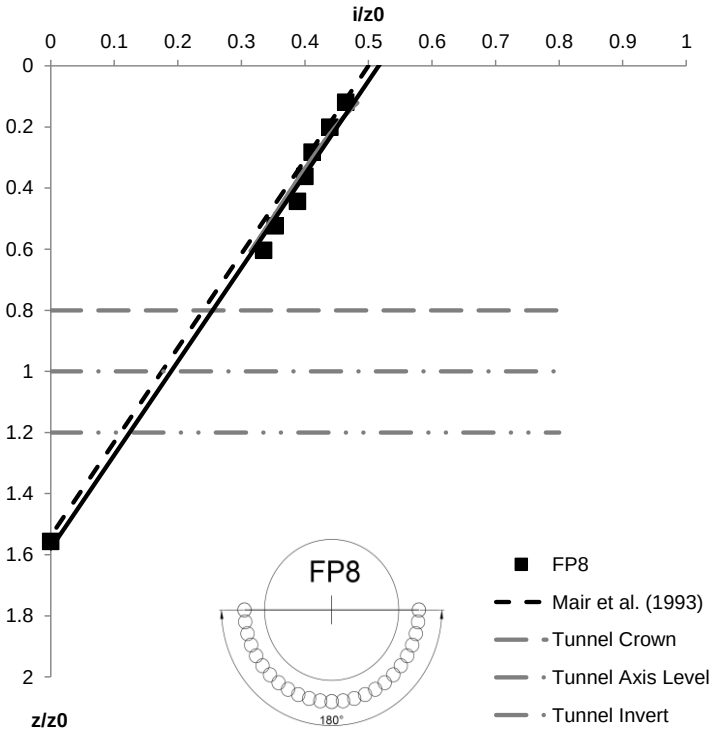

Figure 17: Patterns of deformations with depth for FP8 against theoretical and reference test values

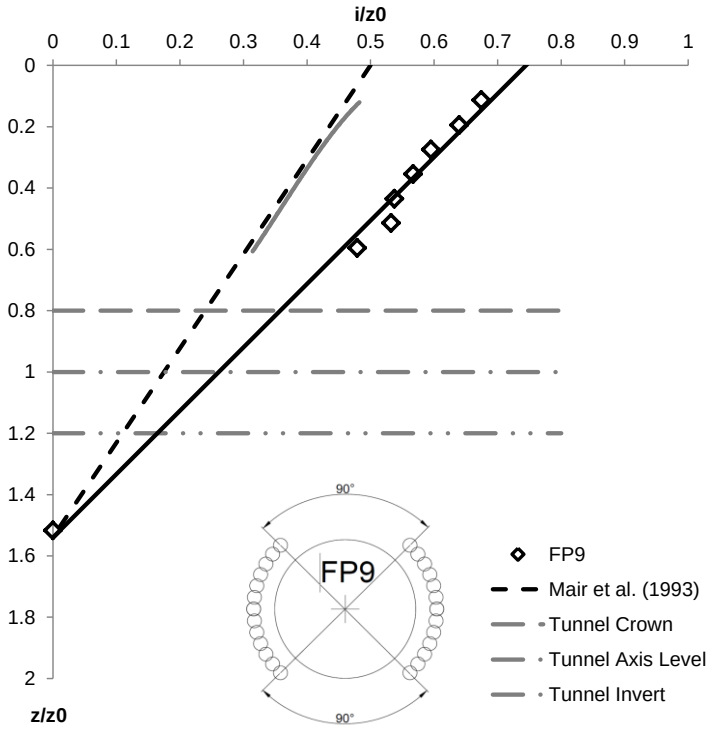

Figure 18: Patterns of deformations with depth for FP9 against theoretical and reference test values